ELSEVIER

Polymer 43 (2002) 4111–4122

polymer

www.elsevier.com/locate/polymer

Glass transition and structural relaxation in semi-crystalline poly(ethylene terephthalate): a DSC study

N.M. Alves[a], J.F. Mano[a], E. Balaguer[b], J.M. Meseguer Dueñas[c], J.L. Gómez Ribelles[b,*]

[a]*Department of Polymer Engineering, Universidade do Minho, Campus de Azurém, 4800 Guimarães, Portugal*
[b]*Department of Applied Thermodynamics, Center for Biomaterials, Universidad Politécnica de Valencia, P.O. Box 22012, E-46071 Valencia, Spain*
[c]*Department of Applied Physics, Center for Biomaterials, Universidad Politécnica de Valencia, P.O. Box 22012, E-46071 Valencia, Spain*

Received 26 June 2001; accepted 5 April 2002

Abstract

The aim of this work is to determine the relaxation times of the cooperative conformational rearrangements of the amorphous phase in semi-crystalline poly(ethylene terephthalate) (PET) and compare them with those calculated in amorphous PET. Samples of nearly amorphous polymer were prepared by quenching and samples with different crystallinity fractions were prepared from the amorphous one using cold crystallisation to different temperatures. The differential scanning calorimetry (DSC) thermograms measured on samples rapidly cooled from temperatures immediately above the glass transition show a single glass transition which is much broader in the case of high-crystallinity samples than in the amorphous or low-crystallinity PET. To clarify this behaviour, the samples were subjected to annealing at different temperatures and for different periods prior to the DSC measuring heating scan. The thermograms measured in samples with low crystallinity clearly show the existence of two amorphous phases with different conformational mobility, these are called Phases I and II. Phase I contains polymer chains with a mobility similar to that in the purely amorphous polymer, while Phase II shows a much more restricted mobility, probably corresponding to conformational changes within the intraspherulitic regions. The model simulation allows to determine the temperature dependence of Phase II relaxation times, which are independent from the crystallinity fraction in the sample and around two decades longer than those of the amorphous polymer at the same temperature.

Keywords: Semi-crystalline poly(ethylene terephthalate); Glass transition; Structural relaxation

1. Introduction

The conformational mobility of the polymer chains pertaining to the amorphous phase of a semi-crystalline polymer is restricted in the proximity of the crystallites and, as a consequence, the glass transition in semi-crystalline polymers depends on the crystalline fraction and also on its microstructure [1–4]. Poly(ethylene terephthalate) (PET) can be easily obtained as either closely amorphous or semi-crystalline, in a range of crystallinities that can range from ~0 to 50% as a result of thermal treatments above the glass transition. Schmidt-Rohr et al. [5] tried to prepare completely amorphous PET by quenching it from the melt into liquid nitrogen, but they always found a residual crystallinity of $5 \pm 2\%$. They also referred that the low-trans probability in the melt could be the primary reason for the relatively low-crystallisation rate of PET, which allows easy preparation at different crystallinity degrees [5]. As the crystallinity of PET may be controlled by different thermal treatments, this material has been frequently used as a model system for studying the influence of crystallinity on the glass transition of the amorphous phase and other physical properties [6–26].

Several techniques such as dielectric spectroscopy [11,21], thermally stimulated depolarisation currents [24], thermally stimulated polarisation currents [24] and dynamic mechanical experiments [17] have been used to reveal the existence of two distinct amorphous phases in PET. Differential scanning calorimetry (DSC) has been specially useful to study the presence of these two phases due to the possibility of performing experiments after subjecting the sample to different thermal treatments that induce physical ageing.

An amorphous polymer (or an amorphous phase in a semi-crystalline polymer) in the glassy state is out of thermodynamical equilibrium, and under constant environmental conditions (in particular at constant temperature and pressure) suffers a process tending to approach equilibrium.

* Corresponding author.

0032-3861/02/$ - see front matter
PII: S0032-3861(02)00236-7

During this process, called physical ageing or structural relaxation the enthalpy, entropy, volume and other physical properties change continuously. A sample that has been subjected to an isothermal treatment at a temperature T_a, in the range or below the glass transition, for a time t_a, and then to a heating scan in the DSC from a temperature well below T_a to a temperature above the glass transition, shows in the thermogram a peak in the interval of the glass transition whose height and temperature location depends on the values of T_a and t_a. The presence of these ageing peaks in the thermogram can be detected much easier than a step in the heat flow or the heat capacity, even if the amount of the amorphous phase responsible for the glass transition is small. This feature has been used in the case of the study of the glass transition of semi-crystalline PET. Double peaks are found in the thermograms of low-crystallinity samples previously annealed at temperatures in the range of the glass transition revealing the presence of two amorphous phases [10,16,17,22,24,25,27], one of them corresponding to the amorphous chains situated close to the crystallites or in intraspherulitic regions and the other in interspherulitic regions.

The study of structural relaxation may provide a deeper insight in the phenomenology of the conformational mobility of the amorphous chains. Structural relaxation is a non-linear and non-exponential process [28–34] and this makes that there is not a simple relationship between the measurable properties and the variables characterising the kinetics of the process, such as the relaxation time. Nevertheless it has been shown that the main features of the structural relaxation process can be modelled on the basis of a distribution of relaxation times that depends both on the temperature and on the structure of the material represented by the value of the relaxing variable (in DSC experiments enthalpy or entropy) [30–39]. A comparison between computer simulation and experimental results allows us to determine a series of parameters than can be in some way related to the molecular mobility.

The evolution of the enthalpy in response to a thermal history consisting of a series of temperature jumps from T_{i-1} to T_i at time instants t_i, followed by isothermal stages is given by

$$H(t) = H^{eq}(T(t)) - \sum_{i=1}^{n} \left(\int_{T_{i-1}}^{T_i} \Delta c_p(T)\, dT \right) \phi(\xi - \xi_{i-1}) \quad (1)$$

where $\Delta c_p(T) = c_{pl}(T) - c_{pg}(T)$ is the configurational heat capacity, the difference between the heat capacity in the equilibrium liquid state and that of the glassy state and ξ is the reduced time:

$$\xi = \int_0^t \frac{dt'}{\tau(t')} \quad (2)$$

The relaxation function ϕ is assumed of the Kohlrausch–Williams–Watts [40] type in most applied models:

$$\phi(\xi) = \exp(-\xi^{\beta}) \quad (3)$$

The relaxation time $\tau(t)$ in Eq. (2) is a function of both temperature and the separation from equilibrium measured by the fictive temperature, which links any out-of-equilibrium state at temperature T with an equilibrium state [30,31]. The fictive temperature T_f can be calculated from enthalpy data through

$$\int_{T_f}^{T^*} (c_{pl}(T) - c_{pg}(T))\, dT = \int_{T}^{T^*} (c_p(T) - c_{pg}(T))\, dT \quad (4)$$

where T^* is a temperature above the glass transition.

In the model proposed by Narayanaswamy [30] and then by Moynihan and co-workers [31] (hereafter the NM model), the double dependence of the relaxation time on temperature and structure is expressed by

$$\tau(T, T_f) = A \exp\left(\frac{\Delta h^*}{R} \left(\frac{x}{T} + \frac{1-x}{T_f} \right) \right) \quad (5)$$

x is a parameter between 0 and 1. Eq. (5) reduced to an Arrhenius dependence for the relaxation time in equilibrium ($T_f = T$) with Δh^*, an apparent activation energy.

Alternatively, in the model proposed by Scherer [33] and Hodge [34] (hereafter called SH model), an expression deduced from the Adam–Gibbs [41] theory is applied

$$\tau(T, S_c) = A \exp\left(\frac{B}{T S_c(\xi, T)} \right) \quad (6)$$

where S_c is the configurational entropy. Assuming $\Delta c_p(T) = T_g \Delta c_p(T_g)/T$, one arrives to [28]

$$\tau(T, T_f) = A \exp\left(\frac{D}{RT(1 - T_2/T_f)} \right) \quad (7)$$

where T_2 is the Gibbs–DiMarzio [42] transition temperature. Eq. (7) reduces to a Vogel equation in equilibrium.

In both NM and SH models, four parameters describe the structural relaxation process (Δh^*, x, A, and β in NM model and D, T_2, A, and β in SH model). These parameters are assumed to be material parameters, and so independent from the thermal history. Nevertheless, it has been shown that it is difficult to reproduce with a single set of model parameters the $c_p(T)$ curves measured in DSC heating scans after different thermal histories [43–46].

One of the main assumptions in the models explained earlier is that an amorphous material kept in isothermal conditions in any out-of-equilibrium state would reach at infinite time an equilibrium state determined by the extrapolation to temperatures below T_g of the enthalpy equilibrium line determined at temperatures above the glass transition. This comes from the identification of the limit of the fictive temperature at infinite time with T. Recently, a model has been proposed in which the limit at infinite time

of the structural relaxation process is considered to be a metastable state with higher configurational entropy and enthalpy than the equilibrium state obtained by extrapolation. This situation would come from the collapse of the configurational rearrangements when the number of configurations available for the polymer segments attains a certain limit. When this limit is reached, the system is in a metastable state and no further decrease in the configurational entropy is possible. Thus, the equilibrium states would not be attainable with the kind of processes described in this work.

To introduce this hypothesis, the model equations were expressed in terms of configurational entropy [38,39,47,48]

$$S_c(t) = S_c^{lim}(T(t)) - \sum_{i=1}^{n}\left(\int_{T_{i-1}}^{T_i} \frac{\Delta c_p^{lim}(T)}{T} dT\right)\phi(\xi - \xi_{i-1}) \quad (8)$$

where $S_c^{lim}(T)$ is the configurational entropy in the metastable limit states. In order to describe this function, it is necessary to introduce new model parameters, something which in principle is not desirable. To reduce the number of new parameters to a minimum $S_c^{lim}(T)$ was defined as shown in Fig. 1(a) (dashed-dotted line). The slope of the $S_c^{lim}(T)$ curve is smaller than the one of the configurational entropy in equilibrium $S_c^{eq}(T)$ at temperatures below the glass transition. The change of slope approaching the equilibrium values is gradual, covering a temperature interval of 15 K. The change of slope shown in the sketch of Fig. 1(a) and determined by the reference temperature, T_{ref}, should be to a certain extent coincident with the glass transition temperature interval. In the calculations, we will take a value for T_{ref} equal to the glass transition temperature determined from the intersection of the enthalpy lines corresponding to the liquid and glassy states. In this way, a single additional parameter δ defined in Fig. 1, is introduced into the model.

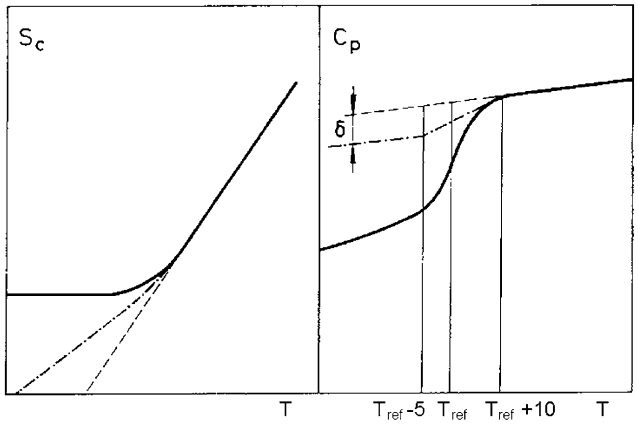

Fig. 1. (a) Sketch of the configurational entropy corresponding to the liquid state (dashed line) to an experimental cooling scan at a finite cooling rate (solid line) and to the hypothetical line of the limit states of the structural relaxation process (dashed-dotted line). (b) $c_p(T)$ lines corresponding to the three cases described in (a). The dashed line corresponds to the liquid state $c_{pl}(T)$, the solid line corresponds to an experimental cooling scan and the dashed-dotted line corresponds to the specific heat capacity in the limit states of the structural relaxation process: $c_p^{lim}(T)$.

In Eq. (8), the reduced time is given by Eq. (2), the relaxation function is the KWW Eq. (3) and the relaxation time is given by the Adam–Gibbs expression (6) which needs no further manipulation to be introduced in Eq. (8).

$\Delta c_p^{lim}(T)$ is defined through

$$S_c^{lim}(T_i) - S_c^{lim}(T_{i-1}) = \int_{T_{i-1}}^{T_i} \frac{\Delta c_p^{lim}(T)}{T} dT \quad (9)$$

thus, if T^* is a temperature above the glass transition region for any temperature T in the glass transition temperature interval or below

$$S_c^{lim}(T) = S_c^{eq}(T^*) + \int_{T^*}^{T} \frac{\Delta c_p^{lim}(T)}{T} dT \quad (10)$$

$$S_c^{eq}(T) = \int_{T_2}^{T} \frac{\Delta c_p(T)}{T} dT \quad (11)$$

It has been shown [38,39,47–50] that the agreement between the model simulation and the experiments is highly improved when the values of $S_c^{lim}(T)$ are significantly higher than those of $S_c^{eq}(T)$.

2. Experimental

The DSC experiments were performed in a Perkin–Elmer DSC7 differential scanning calorimeter with a controlled cooling accessory. The temperature of the equipment was calibrated with indium and lead standards and only the same indium sample was used for the heat flow calibration. The calibrations were performed during heating at 20 °C min^{-1}.

The PET bar, 1 mm thick, was supplied by Goodfellow (catalogue number ES303010). The same sample, with a weight of 20.019 mg, was used in all experiments. This sample was subjected to different thermal treatments with the purpose of obtaining distinct crystallinity degrees.

The 'amorphous' PET was prepared by quenching the sample into cold water, after its melting. All the posterior treatments were carried out in the DSC7 calorimeter. The PET131 was prepared by heating the amorphous sample from 30 to 131 °C at 20 °C min^{-1}. At this temperature, the DSC scan reached 19% of the total crystallisation peak area. Then the sample was cooled at 40 °C min^{-1} (the faster rate for a controlled cooling) from this temperature to the glassy state. PET133, PET135 and PET163 were prepared in a similar way as PET131, the only

difference being the temperature where the heating was interrupted, respectively, 133, 135 and 163 °C, corresponding to partial areas of the crystallisation peak of 31, 47 and 100%. For PET163, the sample was kept at this temperature for 1 h.

Thermal histories included isothermal annealing at different temperatures, T_a, over different times, t_a, after the cooling at 40 °C min^{-1} from the equilibrium rubbery state. The aged samples were then cooled at 40 °C min^{-1} down to 30 °C and the measuring scans were carried out during subsequent heating scans at a constant heating rate of 20 °C min^{-1} until a temperature around 100 °C was reached. This final temperature is such that subsequent crystallisation was prevented although it enabled the obtention of sufficient points in the liquid (rubbery) zone.

3. Results

The thermogram measured in a heating DSC scan on a sample of amorphous PET cooled at 40 °C min^{-1} from a temperature above the glass transition (what we will call the reference scan) shows the glass transition as a step in the specific heat capacity $c_p(T)$, covering a temperature interval from 60 to 80 °C. The glass transition temperature, defined as the temperature of the midpoint of the rise of c_p in the transition, is 71 °C.

The glass transition of the sample crystallised at 135 or 163 °C, which are the samples with the highest crystallinity in this work, is quite different from that of amorphous PET. Roughly speaking, it can be said that it covers the temperature interval between 70 and 110 °C. It is very difficult to give an accurate figure to characterise the glass transition temperature of the semi-crystalline polymer.

The behaviour of the sample crystallised at 131 °C with the lowest crystallinity is similar to that of the amorphous PET, while the thermograms of the samples crystallised at 133 °C are similar to those of the samples crystallised at 135 or 163 °C (Fig. 2).

Figs. 3–6 contain some significant examples of the results obtained after annealing at temperatures in the glass transition range or below it. It is shown that both in amorphous

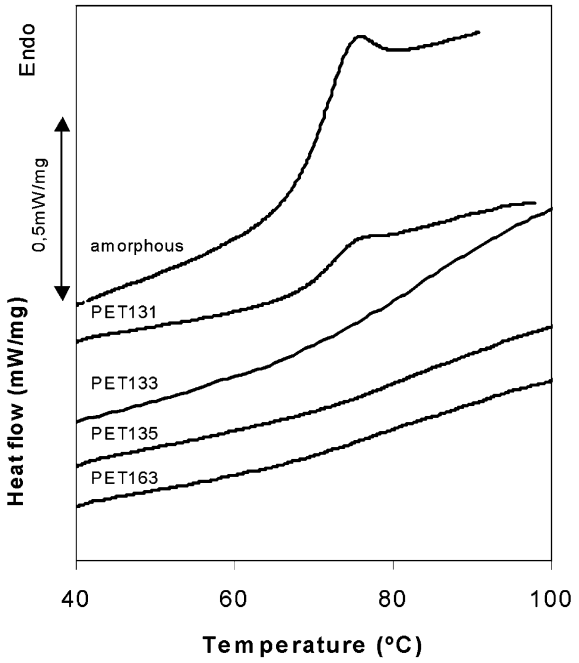

Fig. 2. Thermograms obtained on heating scans on samples of amorphous PET and PET crystallised at 131, 133, 135 and 163 °C. Previously to the scan, the samples were cooled at 40 °C min^{-1} from around 100 °C.

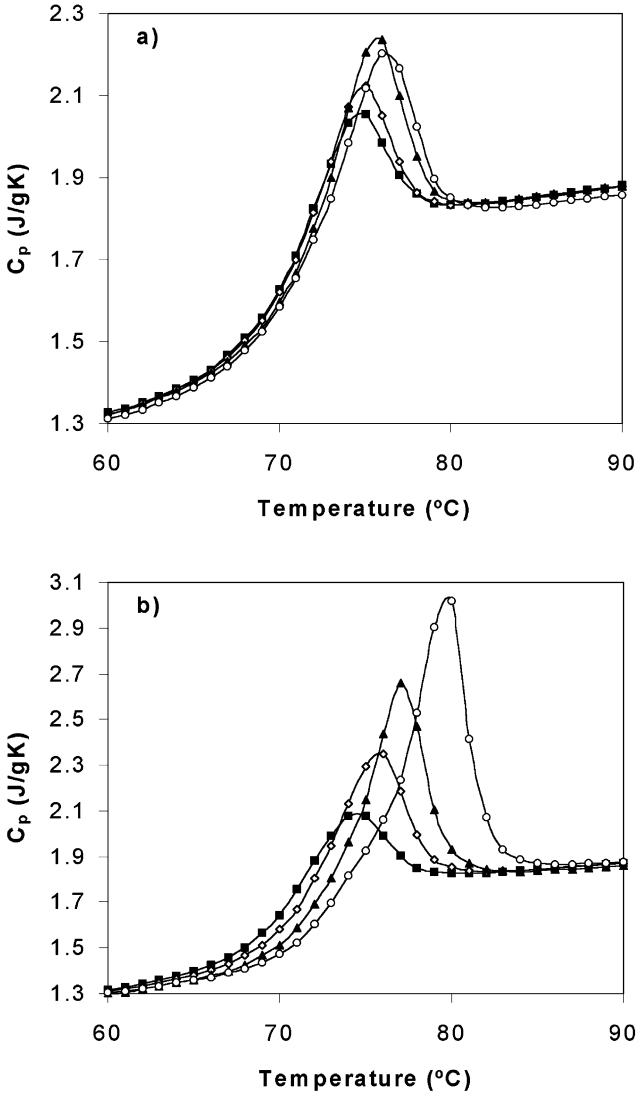

Fig. 3. Temperature dependence of the heat capacity measured in heating DSC scans on samples of amorphous PET subjected to isothermal annealings. (a) Thermograms measured after annealing at 55 °C for (■) 15, (◇) 60, (▲) 240, (○) 3855 min. (b) Thermograms measured after annealing at 62 °C for (■) 5, (◇) 10, (▲) 60, and (○) 120 min (annealings for times longer than 120 min yield exactly the same thermogram, showing that after this time and at this temperature, the sample arrives to a limit stable state).

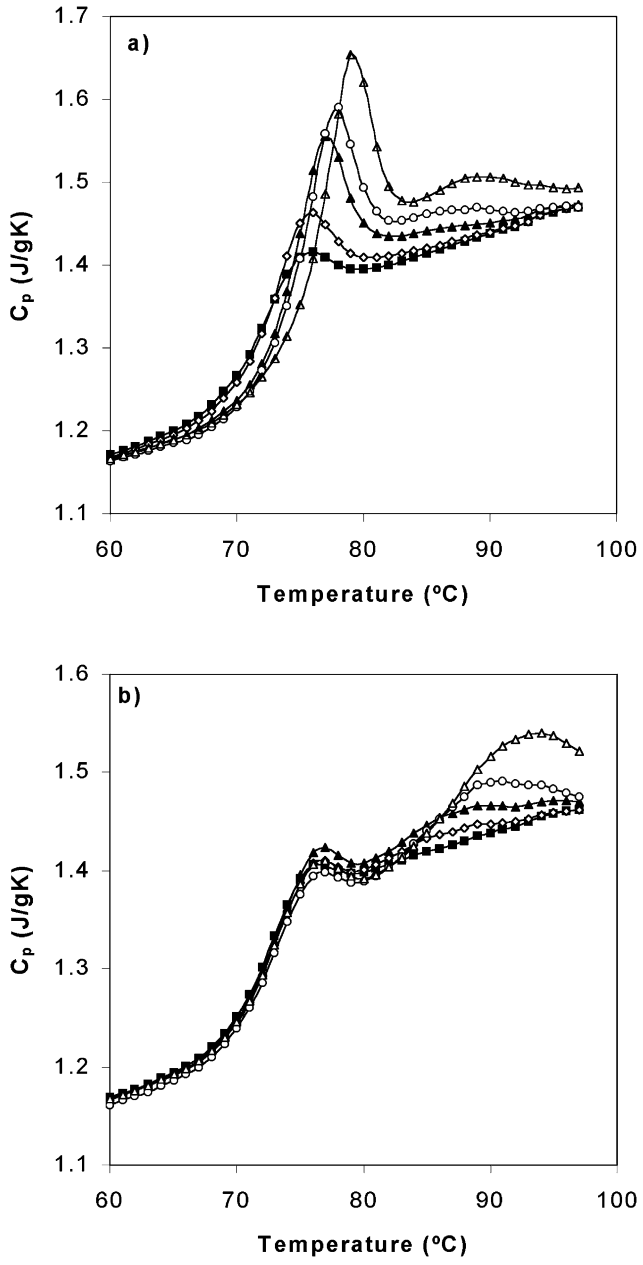

Fig. 4. The temperature dependence of heat capacity measured in heating DSC scans on PET131 sample subjected to isothermal annealing. (a) Thermograms measured after annealing at 54 °C for (■) 10, (◇) 30, (▲) 120, (○) 300, and (△) 1020 min. (b) Thermograms measured after annealing at 62 °C for (■) 10, (◇) 30, (▲) 60, (○) 240, and (△) 1020 min.

PET (Fig. 3) and semi-crystalline samples PET131, PET133 and PET163 (Figs. 4–6), the annealing produces a peak in $c_p(T)$ shifting towards higher temperatures and increasing in height as the annealing time increases. This shift towards higher temperatures happens because the mobility of the chain segments, which are necessary to promote the recovery of enthalpy, decreases during the ageing process. The magnitude of the peak was an indirect measure of the relaxation of enthalpy during the ageing process [51,52]. The curves obtained in PET135 are similar to those of

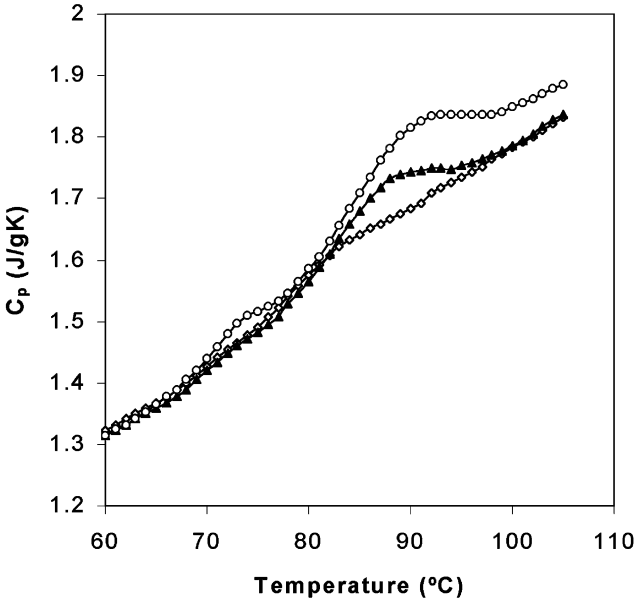

Fig. 5. Temperature dependence of the heat capacity measured in heating DSC scans on samples of PET133 subjected to isothermal annealing at 60 °C for (◇) 30, (▲) 300, and (○) 845 min.

PET163 and are not shown. The peak in the case of PET163 is much broader than in amorphous PET.

4. Discussion

The shape of the thermograms measured in amorphous PET is as expected for an amorphous polymer with a relatively narrow glass transition temperature interval.

Broad glass transitions can be due to a broad distribution of relaxation times, or a low-apparent activation energy around the glass transition temperature. But they can also be produced by the composition heterogeneity of the material as can be the case of polymer blends in which different domains in the material have different composition and thus, different T_g.

The broadening of the glass transition for semi-crystalline PET was also detected by dielectric spectroscopy [4]. These authors observed that only the low-frequency side of segmental mobility is influenced by the presence of the crystalline regions, which agrees with the concept of co-operativity length [53]. The high-frequency side is not influenced by the crystal-imposed geometrical restrictions because of the corresponding short mode length. Their results support the idea of a cooperative glass transition [21,54], where the high-frequency and the low-frequency tails are mainly determined by short range modes and long range modes, respectively.

In miscible blends and IPNs that present a single but very broad glass transition [55,56], it has been reported that the annealing produces a relatively narrow peak in the DSC thermogram. In that case, the sample consists of a

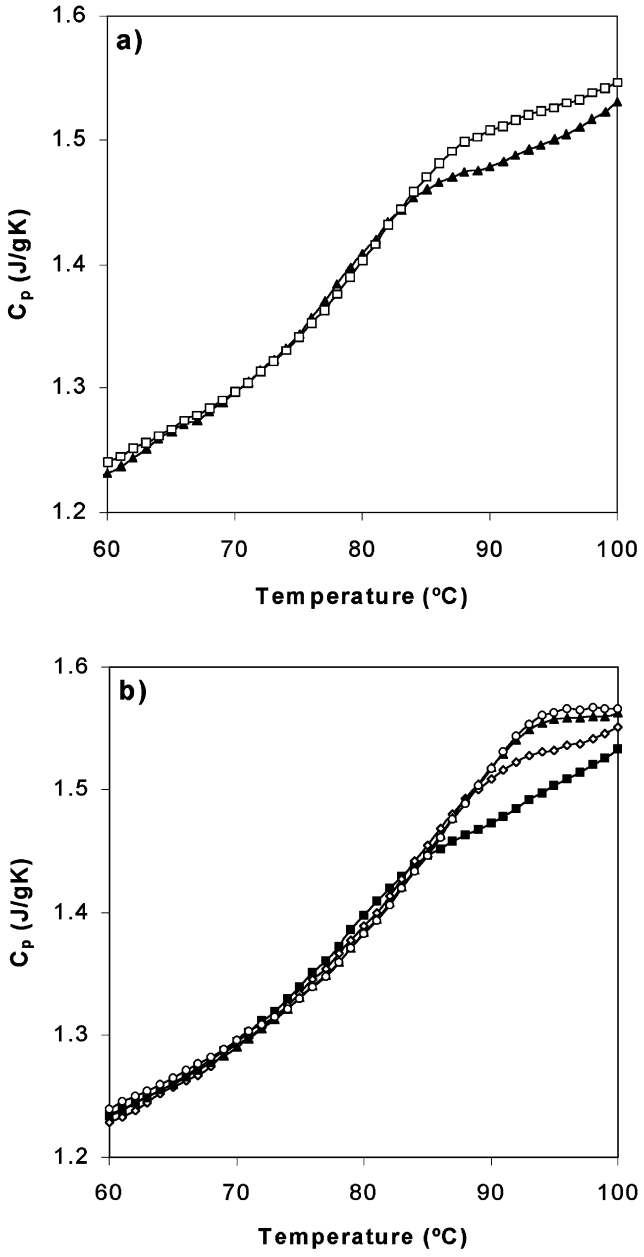

Fig. 6. Temperature dependence of the heat capacity measured in heating DSC scans on samples of PET163 subjected to isothermal annealings. (a) Thermograms measured after annealing at 55 °C for (▲) 240, (□) 768 min. (b) Thermograms measured after annealing at 63.2 °C for 33, 300, 768 and 1200 min.

continuous distribution of regions with different compositions and consequently different glass transitions. When the sample is annealed at a fixed temperature T_a those regions with T_gs below T_a do not relax because they are in equilibrium at that temperature, while those with a T_g higher than say $T_a + 40$ °C have a very small contribution due to their slow structural relaxation. Thus, the response to the thermal treatment, which can be characterised by the peak measured in the heating scan corresponds only to a part of the material.

In the case of the amorphous part of highly crystalline PET, this seems not to be the case. The annealing of the sample at a temperature within the interval in which the glass transition takes place, or immediately below, produces a broad peak in the heating thermogram which covers the whole temperature interval of the glass transition (as shown in Fig. 6). This behaviour seems to be a consequence of a particular kinetics of the structural relaxation of the amorphous part of the semi-crystalline PET that should be quite different from that in the amorphous PET. The modelling of the process will allow a characterisation of the kinetics of the structural relaxation of highly crystalline PET.

The experimental $c_p(T)$ curves measured in PET131 are a clear indication of two differentiated amorphous phases present in semi-crystalline PET, one of them with a glass transition temperature close to that of amorphous PET (we will call it Phase I) and the other one with a higher T_g (Phase II). After annealing at 54 °C, the thermograms show two peaks; the one appearing at the lower temperatures falls in the same region than those appearing in the amorphous PET, while the peaks appearing at the highest temperature fall in the same region than those of PET163. This behaviour agrees with the results reported in the literature for low-crystallinity PET [16,20,22,23]. The appearance of two peaks after annealing at a temperature T_a means that at this temperature both amorphous phases are out of thermodynamical equilibrium and experience the structural relaxation process. The rate of this process greatly depends on the difference between T_a and the glass transition temperature. Thus at $T_a = 54$ °C (Fig. 4(a)), the structural relaxation process of Phase I is quicker than that of Phase II and the low-temperature peak shown in the heating thermogram is consequently higher. At 62 °C, Phase I is very close to equilibrium and the evolution of the enthalpy during annealing is small, as can be seen in the results obtained on amorphous PET annealed at this temperature. On the contrary, at this temperature Phase II suffers an important evolution which is detected by the dependence of both the peak height and the temperature of the maximum with annealing time. Something similar also occurs in PET163 at the same temperature (Fig. 6).

PET133 shows a behaviour very similar to PET163, but after some specific treatments such as annealing for long periods of time at 60 °C (Fig. 5), a very small peak is shown in the heating thermogram around 75 °C in addition to the main peak appearing between 80 and 100 °C as in the other samples with higher crystallinity.

Our results support the idea that the amorphous part of the semi-crystalline PET is organised in two phases. The origin of these two phases should be consistent with the spherulitic morphology of this polymer, in which crystalline lamellae, amorphous layers between the lamellae and amorphous regions between the growing spherulites [17] coexist. Phase I is far enough from the crystallites to be able to undertake conformational rearrangements as in the fully amorphous polymer. Phase II would be formed by polymer

Table 1
Configurational heat capacity at T_g of amorphous and semi-crystalline PET and the model parameters determined by the least-squares routine under the assumption $S_c^{lim}(T) = S_c^{eq}(T)$. The glass transition temperature for the different samples calculated at the temperature at which the relaxation time in equilibrium is 100 s is also included. See text

	B (J/g)	Δc_p (J/g K)	β	T_2 (°C)	ln(A/s)	$T_g(\tau^{eq} = 100\ s)$, $S_c^{lim}(T) = S_c^{eq}(T)$	Δh^* (kJ/mol)	x
Amorphous PET	1000	0.33	0.41	−10.4	−31.4	65	350	0.46
PET133	580	0.19	0.26	6.5	−29.4	87	470	0.34
PET135	360	0.12	0.25	−1.9	−27.2	82	440	0.36
PET163	400	0.13	0.22	13.7	−30.2	92	540	0.30

chains that are located between crystalline lamellae with consequent restricted mobility. In fact the dynamics of the conformational mobility of macromolecules has been shown to be dependent upon the confinement of the corresponding phase [57,58]. Phase I is predominant in low-crystallinity PET131, while in the PET with higher crystallinity nearly the whole amorphous phase has constrained mobility and form the Phase II, as proved by the fact that nearly no low-temperature glass transition is detected in PET133, PET135 and PET163 with the exception of very small traces in PET133. If we accept that the length of cooperativity at the glass transition temperature is around a few nanometers, these results support that in PET133, PET135 and PET163 there are no regions of this dimensional scale consisting of polymer chains with unconstrained mobility.

Model simulation of the thermal treatments to which the sample is subjected in the DSC scans allows estimating the relaxation times of the conformational rearrangements producing structural relaxation. Model equations include the temperature dependence of the configurational specific heat $\Delta c_p(T)$. A linear equation for $\Delta c_p(T)$ has been shown to reproduce accurately the experimental results in amorphous polymers [59]. In our experiments, the experimental results contain few information about the heat capacity of the samples in liquid state, as the highest temperature of the scans is not far from the glass transition in order to avoid any crystallisation of the sample. In the model calculations, we will use a constant value for Δc_p. To calculate it, the heat capacity of the glass was fitted to a straight line determined by least-squares in the temperature interval between 30 and 60 °C. The specific heat of the liquid was consider as a straight line with the same slope than the one of the glass but coinciding with the experimental value of c_p at 110 °C. This determines the values Δc_p that are included in Table 1.

As a first step, computer simulation was conducted under the assumption that the limit state of the structural relaxation coincides with the extrapolated equilibrium states, i.e. with parameter $\delta = 0$ in the model equations. Thus, the model is quite similar to SH model (the model called AGL by Hodge [34]). Five thermograms corresponding to five different thermal histories were selected for each sample.

Due to the correlation existing between the parameters B and T_2 in the model equations, least-squares routine was conducted with a fixed value of B, looking for the set of three parameters β, T_2 and A minimising the sum of the error function of the five thermograms. In this way, the least-squares routine looks for a single set of parameters, characteristic of the material but independent from thermal histories. The procedure was repeated with different values of B. For $B = 1000$ J/g, the value of A found by the search routine for amorphous PET was 10^{-14} s and the difference was $T_g - T_2 \approx 75$ °C. These values are in the order of what should be expected for the glass transition behaviour of the amorphous polymers. If the value of B is higher, the pre-exponential factor A and the difference $T_g - T_2$ rapidly decrease to unrealistic values. The results of the fits conducted with $B = 1000$ J/g are shown in Fig. 7 and Table 1.

In the case of amorphous PET, the fit is quite satisfactory taking into account that all the thermograms are reproduced with the same set of parameters (Fig. 6).

In the case of the semi-crystalline samples, the glass transition and the structural relaxation phenomena are due only to a part of the polymer sample. As a consequence, the value of the configurational heat capacity, Δc_p, is smaller than in the amorphous sample and the same occurs with the configurational entropy which is proportional to Δc_p. In this way, the same set of model parameters (which means the same mobility of the amorphous chains) would predict according to Eq. (6), much larger values of the relaxation times in the semi-crystalline polymer than in the amorphous one. To take this into account, the curve fitting procedure was conducted in the semi-crystalline samples with values of B such as $B/\Delta c_p$ being the same as in the amorphous PET: $B/\Delta c_p = 1000/0.32 = 3.125$ kK. The values of the parameter B for each sample are included in Table 1. This procedure ensures that the relaxation times calculated by the model are representative of the conformational mobility of the part of the polymer which is responsible for the structural relaxation.

The model calculation under the assumption $S_c^{lim}(T) = S_c^{eq}(T)$ yields in the case of semi-crystalline samples two $c_p(T)$ curves with peaks taller and narrower than the experimental ones, but with maxima quite coincident with the experiment, as shown in Fig. 8 for PET133. The curves are completely analogous in the PET135 and PET163. No attempt was made to simulate the results of PET131 since

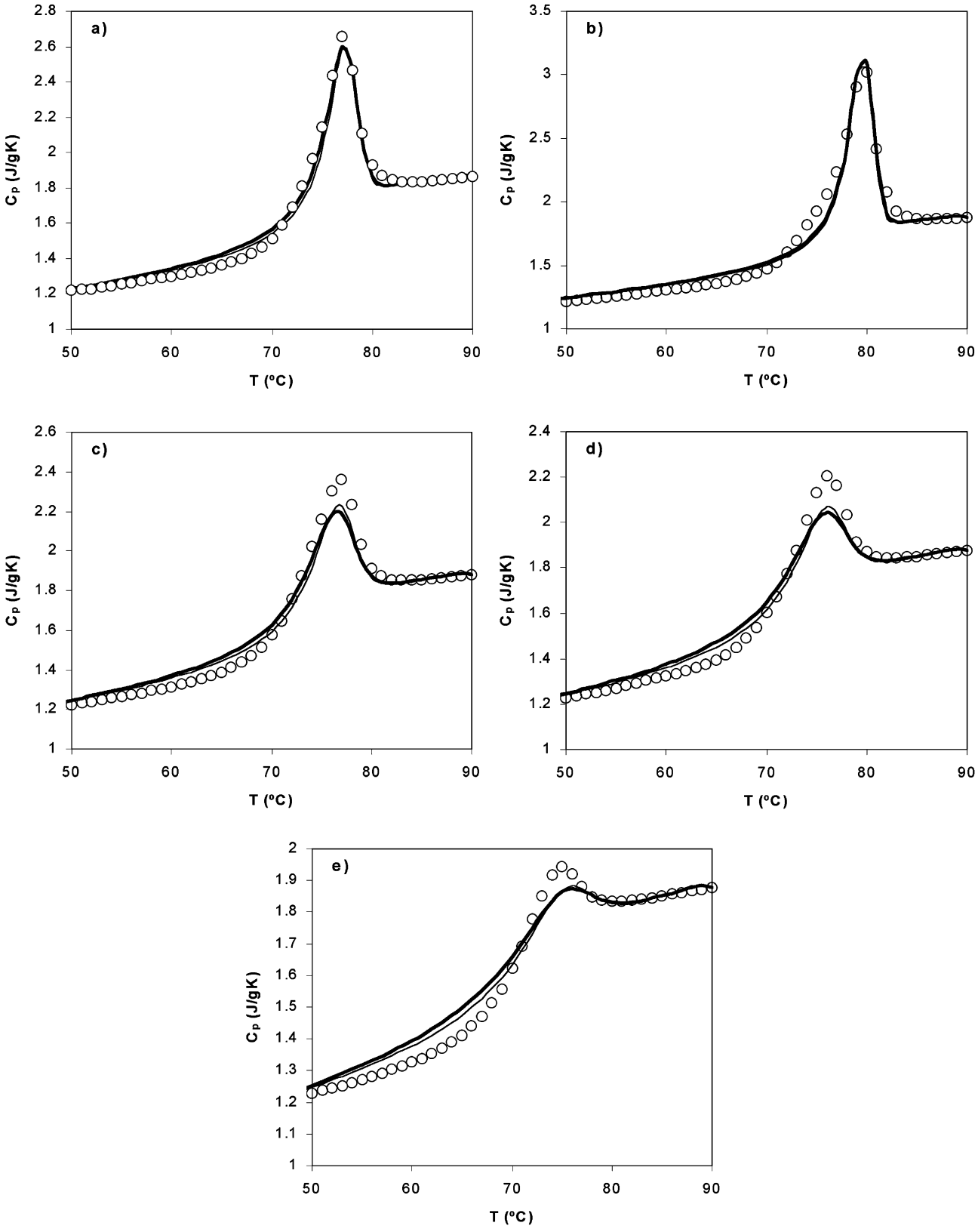

Fig. 7. Temperature dependence of the heat capacity of amorphous PET measured after different thermal treatments (open circles). (a) $T_a = 55$ °C, $t_a = 240$ min, (b) $T_a = 55$ °C, $t_a = 3855$ min, (c) $T_a = 60$ °C, $t_a = 600$ min, (d) $T_a = 62$ °C, $t_a = 855$ min, (e) $T_a = 67$ °C, $t_a = 120$ min. The narrow line represents the curves calculated under the assumption $S_c^{lim}(T) > S_c^{eq}(T)$ the parameters according to Table 2. The thick line represents the curves calculated with $S_c^{lim}(T) = S_c^{eq}(T)$, and the parameters according to Table 1.

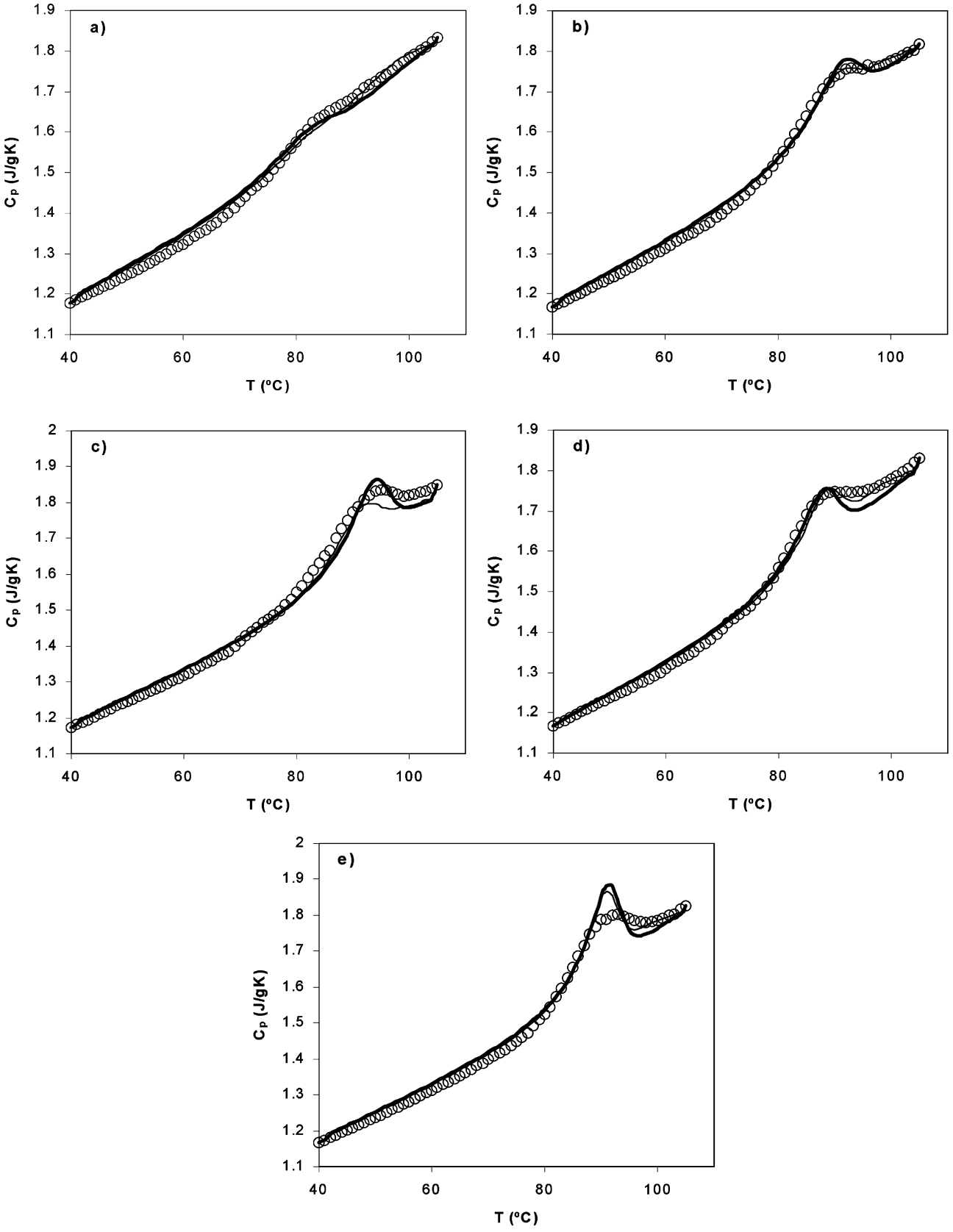

Fig. 8. Temperature dependence of the heat capacity of PET133 sample measured after different thermal treatments (open circles). (a) $T_a = 60$ °C, $t_a = 1800$ min, (b) $T_a = 65$ °C, $t_a = 300$ min, (c) $T_a = 65$ °C, $t_a = 960$ min, (d) $T_a = 55$ °C, $t_a = 940$ min, (e) $T_a = 55$ °C, $t_a = 3780$ min. The narrow line represents the curves calculated under the assumption $S_c^{lim}(T) > S_c^{eq}(T)$ with the parameters according to Table 2. The thick line represents the curves calculated with $S_c^{lim}(T) = S_c^{eq}(T)$, and the parameters according to Table 1.

Table 2
Model parameters determined by the least-squares routine under the assumption $S_c^{lim}(T) > S_c^{eq}(T)$. See text

	B (J/g)	δ (J/g K)	$\delta/\Delta c_p$	β	T_2 (°C)	ln(A/s)
Amorphous PET	1000	0.05	0.15	0.41	−7	−32.9
PET133	580	0.08	0.42	0.29	6	−32.1
PET135	350	0.05	0.40	0.30	−2	−29.5
PET163	400	0.07	0.54	0.36	8	−31.8

the model does not include the presence of two independent glass transitions and so it is not able to reproduce the double peaks appearing in the experimental thermograms. The sets of parameters found are included in Table 1.

Trying to improve the fit, the least-squares routine was conducted in all the samples under the assumption of $S_c^{lim}(T) > S_c^{eq}(T)$. The value of B was fixed and the least-squares routine looked for the set of four parameters β, δ, T_2 and A. The values of the parameters for each sample are in Table 2 and the computed simulated $c_p(T)$ curves are represented in Fig. 7 for the amorphous PET and in Fig. 8 for PET133. The fit in the case of the semi-crystalline samples slightly improves under the assumption of $S_c^{lim}(T) > S_c^{eq}(T)$ but some of the calculated thermograms (the one represented in Fig. 7(e) is an example) still show peaks narrower than the experimental ones. The difference in the model-simulated curves does not justify in this case the introduction of the new parameter δ, and thus the relaxation times will be analysed in terms of the sets of parameters of Table 1, i.e. under the assumption $S_c^{lim}(T) = S_c^{eq}(T)$.

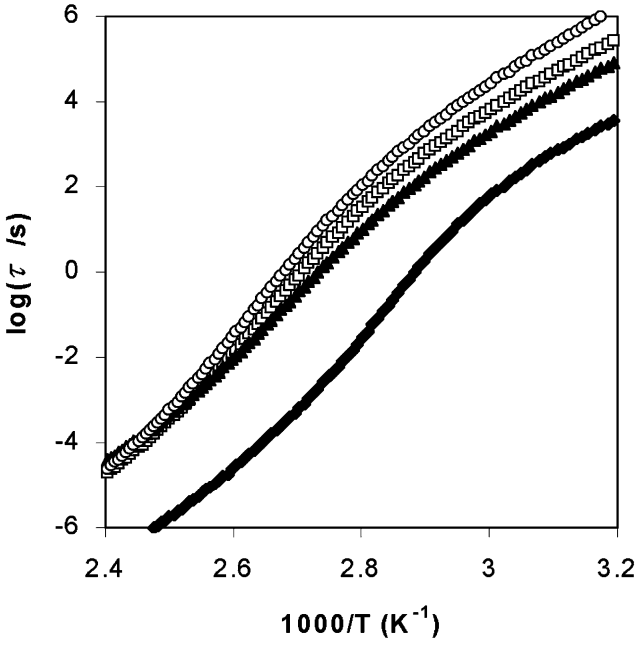

Fig. 9. Temperature dependence of the relaxation times calculated for amorphous (◆) PET, (□) PET133, (▲) PET135, and (○) PET163 during 40 °C min^{-1} cooling. The computer simulation was conducted with the sets of parameters according to Table 1.

The relaxation time was evaluated with the model equations for the cooling of the sample at 40 °C min^{-1} from equilibrium, using the sets of model parameters found by the search routine (Table 1). The results of model simulation are shown in Fig. 9. At high temperature, while the sample is in equilibrium, the relaxation time depends on temperature according to Eq. (12), showing a curvature in the log τ vs $1/T$ similar to that predicted by the Vogel equation

$$\tau^{eq}(T, S_c) = A \exp\left(\frac{B}{TS_c^{eq}(T)}\right) \tag{12}$$

It seems that the equilibrium relaxation times in the semi-crystalline polymers are longer than in amorphous PET for any temperature, or equivalently, that the whole relaxation process is shifted towards higher temperatures in the semi-crystalline PET with respect to the fully amorphous sample. The glass transition temperature can be defined as the temperature at which the relaxation time attains a determined fixed value taken frequently as 100 s [60]. This definition gives us a value of T_g for the semi-crystalline PET that was difficult to determine from the reference scans as mentioned earlier. This value is shown in Table 1.

In the glass transition, this behaviour changes when the material goes into the glassy state. At low temperatures log τ depends linearly on the reciprocal of temperature according to Arrhenius behaviour which is characteristic of the glassy state. This behaviour is a consequence of the configurational entropy being almost independent from temperature in the glassy state (see Eq. (7)). It is remarkable that the log τ curves calculated for the semi-crystalline samples are nearly coincident with each other. The slope of the Arrhenius diagram in the glassy state

$$\frac{\mathrm{d}\ln\tau^{glass}}{\mathrm{d}(1/T)} = \frac{E_a^{glass}}{R} \tag{13}$$

allows determining a value for the apparent activation energy E_a^{glass} of 160 ± 3 kJ/mol for both amorphous and semi-crystalline samples. The consequence is that the value of the configurational entropy in the glassy state is very similar in both amorphous phases. This is not surprising since S_c^{glass} should be a characteristic, nearly universal parameter determining the temperature interval in which the glass transition takes place. This activation energy can be related to the x parameter in HN phenomenology according to Eq. (5)

$$x = \frac{E_a^{glass}}{\Delta h^*} \tag{14}$$

and Δh^* can be calculated from the slope of the equilibrium relaxation time at the glass transition temperature

$$\left.\frac{\mathrm{d}\ln\tau^{eq}}{\mathrm{d}(1/T)}\right|_{T_g} = \frac{\Delta h^*}{R} \tag{15}$$

The values of the parameter x in semi-crystalline PET are

not very different from each other and smaller than in the amorphous sample (Table 1).

The value of the parameter β is not exactly the same in all the semi-crystalline samples. Nevertheless, it is always smaller in the semi-crystalline PET than in the amorphous sample, indicating that the distribution of relaxation times is broader. The close interaction with crystallites smoothens the process of finding amorphous rearranging regions with different mobility.

The values of the β parameter are concordant with values obtained by other authors [11,21]. The changes observed in the α dielectric relaxation process during crystallisation [21] were fitted by the KWW equation. The β_{KWW} parameter of this equation decreased from 0.3 (amorphous) to 0.21 as crystallinity increased.

In Ref. [52], the authors found that the relaxation function of the α relaxation could be fitted by a Havriliak–Negami equation (in the frequency domain) or by a KWW equation (in the time domain) at the initial stage of crystallisation. In the same study [11], the β_{KWW} parameter varied between 0.41 and 0.34 when the crystallisation time increased from 271 to 2952 min. According to the authors [11], at the beginning of the crystallisation the α relaxation was mainly related to the polymer dynamics within the isotropic amorphous phase. Therefore, it was expected that the relaxation behaviour followed the KWW equation as observed in usual amorphous polymers.

5. Conclusions

The mobility of the amorphous phase in semi-crystalline PET can be affected by the proximity of crystallites. When the amount of crystalline phase is small, two amorphous phases with clearly differentiated conformational mobility and consequently with two separated glass transition processes can be distinguished. Phase I shows the glass transition in the same temperature range than amorphous PET and so it can be ascribed to the amorphous conformational rearranging regions which are far from the crystallites. Phase II, showing the glass transition at higher temperatures, could consist of polymer chains close to the crystalline lamellae.

A clear difference has been found between the temperature dependence of the relaxation time of the conformational rearrangements of Phases I and II. The former characterised by the behaviour of amorphous PET. There has been found no correlation between the crystallinity of the sample and the mobility of Phase II. Although there is some scattering in the results found in the different semi-crystalline samples, the mobility of amorphous chains close to the crystallites or linked to them seems to be a characteristic of this interaction and not of the amount of crystalline phase. When the crystallinity of the samples is higher than a critical amount, DSC is not able to detect any conformational motion, which could be ascribed to unconstrained amorphous Phase I.

Acknowledgements

N.M.A. and J.F.M. acknowledge the financial support of Fundação da Ciência e Tecnologia (Project PRAXIS/P/CTM/14171/1998). J.L.G.R. and J.M.M.D. wish to acknowledge the support of CICYT through the MAT97-0634-C02-01 project. Support from the Portuguese–Spanish joint research action (Spain: HP1999-0024; Portugal: E/69/00) is also acknowledged.

References

[1] Struik LCE. Polymer 1987;28:1521.
[2] Shick C, Kramer L, Mischok W. Acta Polym 1985;36:47.
[3] Struik LCE. Physical ageing in amorphous polymers and other materials. Amsterdam: Elsevier, 1978.
[4] Dobbertin J, Hensel A, Schick C. J Therm Anal 1996;47:1027.
[5] Schmidt-Rohr K, Hu W, Zumbulyadis N. Science 1998;280:714.
[6] Sawada K, Ishida YJ. J Polym Sci, Polym Phys Ed 1975;13:2247.
[7] Aref-Azar A, Hay JN. Polymer 1982;23:119.
[8] Berens AR, Hodge IM. Macromolecules 1982;15:756.
[9] Ito E, Tajima K, Kobayashi Y. Polymer 1983;24:877.
[10] Coburn JC, Boyd RH. Macromolecules 1986;19:2238.
[11] Fukao K, Miyamoto Y. J Non-Cryst Solids 1997;212:208.
[12] Belana J, Pujal M, Colomer P, Montserrat S. Polymer 1988;29:1738.
[13] Montserrat S, Cortés P. Makromol Chem Macromol Symp 1989;27:279.
[14] Santa Cruz C, Baltá Calleja FJ, Zachmann HG, Stribeck N, Asano TJ. J Polym Sci, Polym Phys Ed 1991;29:819.
[15] Santa Cruz C, Stribeck N, Zachmann HG, Baltá Calleja FJ. Macromolecules 1991;20:5980.
[16] Montserrat S, Colomer P, Belana J. J Mater Chem 1992;2:217.
[17] Vigier G, Tatibouet J, Benatmane A, Vassoille R. Colloid Polym Sci 1992;270:1182.
[18] Vigier G, Tatibouet J. Polymer 1993;34:4257.
[19] Belana J, Mudarra M, Cañadas JC, Colomer P. J Mater Sci 1993;28:3805.
[20] Itoyama K. Polymer 1994;35:2117.
[21] Ezquerra TA, Baltá-Calleja FJ, Zachmann HG. Polymer 1994;35:12.
[22] Montserrat S, Cortés P. J Mater Sci 1995;30:1790.
[23] Cañadas JC, Diego JA, Mudarra M, Belana J. Polymer 1998;39:2795.
[24] Diego JA, Cañadas JC, Mudarra M, Belana J. Polymer 1999;40:5355.
[25] Zhao J, Song R, Zhang Z, Linghu X, Zheng Z, Fan Q. Macromolecules 2001;30:343.
[26] Dargent E, Cabot C, Saiter JM, Bayard J, Grenet J. J Therm Anal 1996;47:887.
[27] Suzuki H, Grebowicz J, Wunderlich B. Br Polym J 1985;17:1.
[28] Davies RO, Jones GO. Adv Phys 1953;2:370.
[29] Kovacs AJ. Fortschr Hochpolym Forsch 1963;3:394.
[30] Narayanaswamy OS. J Am Ceram Soc 1971;54:491.
[31] Moynihan CT, Macedo PB, Montrose CJ, Gupta PK, DeBolt MA, Dill JF, Dom BE, Drake PW, Esteal AJ, Elterman PB, Moeller RP, Sasabe H. Ann NY Acad Sci 1976;279:15.
[32] Kovacs AJ, Aklonis JJ, Hutchinson JM, Ramos AR. J Polym Sci, Polym Phys Ed 1979;17:1097.
[33] Scherer GW. J Am Ceram Soc 1984;67:504.
[34] Hodge IM. Macromolecules 1987;20:2897.
[35] Scherer GW. J Non-Cryst Solids 1990;123:75.
[36] Hodge IM. J Non-Cryst Solids 1994;169:211.
[37] Hutchinson JM. Prog Polym Sci 1995;20:703.

[38] Gómez Ribelles JL, Monleon Pradas M. Macromolecules 1995;28:5867.
[39] Gómez Ribelles JL, Monleon Pradas M, Vidaurre Garayo A, Romero Colomer F, Más Estellés J, Meseguer Dueñas JM. Polymer 1997;38:963.
[40] Williams G, Watts DC. Trans Faraday Soc 1970;66:80.
[41] Adam G, Gibbs JH. J Chem Phys 1965;43:139.
[42] Gibbs JH, DiMarzio EA. J Chem Phys 1958;28:373.
[43] Prest WM, Roberts Jr. FJ, Hodge IM. Proc NATAS Conf 12th 1980:119–23.
[44] Tribone JJ, O'Reilly JM, Greener J. Macromolecules 1986;19:1732.
[45] Romero Colomer F, Gómez Ribelles JL. Polymer 1989;30:849.
[46] Gómez Ribelles JL, Ribes Greus A, Diaz Calleja R. Polymer 1990;31:223.
[47] Brunacci A, Cowie JMG, Ferguson R, Gómez Ribelles JL, Vidaurre Garayo A. Macromolecules 1996;29:7976.
[48] Meseguer Dueñas JM, Vidaurre Garayo A, Romero Colomer F, Más Estellés J, Gómez Ribelles JL, Monleón Pradas M. J Polym Sci, Polym Phys Ed 1997;35:2201.
[49] Montserrat S, Gómez Ribelles JL, Meseguer Dueñas JM. Polymer 1998;39:3801.
[50] Gómez Ribelles JL, Vidaurre Garayo A, Cowie JMG, Ferguson R, Harris S, McEwen IJ. Polymer 1998;40:183.
[51] Petrie SEB. J Polym Sci Part A-2 1972;10:1255.
[52] Foltz CR, McKinney PV. J Appl Polym Sci 1969;13:2235.
[53] Donth E. Glasübergang. Berlin: Akademieverlag, 1981.
[54] Schönhals A, Schlosser E. Colloid Polym Sci 1989;267:125.
[55] Cowie JMG, Ferguson R. Macromolecules 1989;22:2312.
[56] Gómez Ribelles JL, Meseguer Dueñas JM, Torregrosa C, Monleón Pradas M. DSC results on a poly[methyl acrylate]–poly[methyl methacrylate] interpenetrated polymer network. Submitted for publication.
[57] Pissis P, Kyritsis A, Barut G, Pelster R, Nimtz G. J Non-Cryst Solids 1998;235–237:499.
[58] Schönhals A, Stauga R. J Non-Cryst Solids 1998;235–237:450.
[59] Mathot VBF. Polymer 1984;25:579.
[60] Richert R, Blumen A, editors. Disordered effects on relaxational processes. Berlin: Springer, 1994.